Convoy-electron emission induced by multiple collisions of H^+ and H^0 on a thick He target

D. Fregenal, G. Bernardi, P. Focke, and W. Meckbach
Centro Atómico Bariloche and Instituto Balseiro, Comisión Nacional de Energía Atómica, 8400 Bariloche, Argentina
(Received 18 December 1996)

We present double-differential electron distributions, measured in the neighborhood of the velocity of the emerging projectiles, for 45-keV H^+ and H^0 incident on a He target. Target thicknesses range from single-collision conditions through a multiple-collision regime up to charge equilibrium in the emerging beam. The convoy-electron emission yield is determined as a function of target thickness. Using a simple rate equation and known cross sections for charge exchange and electron scattering, approximate agreement with experiment is obtained. A smaller electron-He scattering cross section improves this agreement. This result could be interpreted as due to the effect of the projectile Coulomb field in the transport of the electrons. [S1050-2947(97)01607-7]

PACS number(s): 34.80.Bm, 34.70.+e

I. INTRODUCTION

The electron emission induced by atomic collisions with gaseous and thin solid foil targets has been the subject of extensive investigations. In particular much interest was devoted to the so-called convoy electrons emitted in the forward direction with a velocity ($\mathbf{v}$) close to that of the emerging projectiles ($\mathbf{v}_p$). This subject has been reviewed in various works [1–4]. As a distinctive feature, a sharp peak, centered at $\mathbf{v}=\mathbf{v}_p$, is observed in doubly differential electron distributions. This peak is considered as due to the final-state electron-ion Coulomb interaction. Under single-collision conditions there are two primary mechanisms for the production of electrons in the continuum of the projectile Coulomb field: electron capture to the continuum (ECC) and electron loss to the continuum (ELC). The former has its origin in target ionization. The latter is produced by ionization of electrons originally bound to the projectile. Recently, coincidence measurements revealed the surprising evidence of convoy electrons emitted into the continuum of neutral projectiles that can find their origin in ECC of incident neutral atoms [5–7].

Experimental studies of convoy-electron production in gas targets have been done only under single-collision conditions. We present here an experiment in which, starting with single collisions of incident protons (H^+) and neutral hydrogen projectiles (H^0), the thickness π, in at./cm^2, of a He gas target is purposely increased. In this way a multiple-collision regime was provoked, leading to charge exchange in the projectile beam and scattering of the electrons produced along the beam path in the target. It was possible to pursue this study up to the attainment of saturation of the emission of convoy electrons, which resulted when dynamic equilibrium of the charge distribution in the emerging projectile beam was reached.

Up to the present, experiments concerning the dependence of convoy-electron emission on target thickness have been performed solely with solid foil targets. For hydrogen projectiles such studies could only be performed at energies above 1 MeV/u, for which the penetration of the projectiles is sufficient to cover the transition into charge equilibrium. However, an observation of the initial rise of convoy-electron emission, which occurs in the range of small thicknesses not accessible with foils, was not possible [8,9].

We remark that, besides the possibility of covering the total range of thicknesses of interest, the reduced atomic density of the gas target determines, on the one hand, well-defined atomic states of the projectiles and, on the other hand, macroscopic mean free paths of the electrons between collisions. This facilitates the applicability of the simple rate equations [4,8–10] for the description of convoy-electron emission yields as a function of target thickness.

II. EXPERIMENT

Our experimental setup, including the electron spectrometer, has been described in detail elsewhere [11]. A magnetically selected proton beam was collimated to 0.4×0.4 mm^2 before entering the collision chamber. A H^0 beam was obtained by charge exchange in a cell placed upstream and subsequent deflection of the remaining charged component. The target gas was fed into a cell with a length of 30 mm, provided with orifices 0.75 mm in diameter for the passage of the projectile beam. The entrance or ''object'' focus of the spectrometer was localized at the exit hole of this cell. As electrons born inside the target cell had also to be measured, it was verified that the acceptance of the spectrometer did not change when analyzing electrons originated up to 30 mm ahead of this focus. This was achieved by replacing the cell by a thin foil target that could be displaced longitudinally through this distance resulting in convoy-electron spectra that were independent of the position of the foil.

The target thickness π (at./cm^2) was determined by a dynamic method: For a known flow of gas, the conductance of the thin circular holes of the target cell permitted one to calculate the pressure in the cell. Gas flows were measured by evacuating a container of known volume (472.4 cm^3) connected to the gas cell; the pressure in this container was registered as a function of time with a capacitance manometer. Simultaneously, the pressure in the collision chamber was registered with an ionization gauge. With this information it was possible to relate the target thickness π directly to this pressure.

The base pressure in the collision chamber was below

10^{-7} Torr. With the target gas ''in,'' the pressure increased from 1.5×10^{-7} Torr up to 2×10^{-5} Torr. This pressure range corresponded to a range in target thicknesses, including corrections that account for the gas escaping through the cell holes, from $\pi=1.5\times10^{14}$ at./cm^2 to 4.3×10^{16} at./cm^2. This represents an increase by more than two orders of magnitude. Statistical uncertainties in the target thickness were of the order of $\pm5\%$. Below $\pi=6\times10^{14}$ at./cm^2 they increased up to $\pm13\%$ for the lowest thickness. These estimates do not include an additional constant error of $\pm9\%$, due to the evaluation of the conductance of the holes in the gas cell.

When measuring electron spectra, the registered electron counts were normalized to the projectile beam collected in a Faraday cup. The incident projectiles had to traverse a thin carbon foil, mounted in front of the cup entrance, in which the beam was charge equilibrated. In this way one obtained a collected beam signal that was independent of the evolution of the charge fractions in the target cell.

III. MEASUREMENTS AND RESULTS

We measured convoy-electron spectra in the forward direction for H^+ and H^0 projectiles at 18 different target thicknesses. The projectile energy $E_p=45$ keV corresponding to a velocity $v_p=1.34$ a.u., was selected in such a way that the attenuation of electrons of velocity v_p ($E\cong25$ eV) by collisions with atoms in the He target was dominated by the elastic scattering channel [12].

In Fig. 1 we show electron spectra for H^+ and H^0 impact, measured at four representative target thicknesses. To facilitate the comparison of the convoy-peak shapes these spectra were normalized to unity at the peak tops.

For the smallest thickness ($\pi=1.5\times10^{14}$ at./cm^2) the electron emission process is dominated by single-collision conditions [13,14]. We see in Fig. 1(a) that the spectrum obtained with incident H^+ exhibits a strong negative skewness, typical of the ECC process. The almost symmetric peak obtained with H^0 is typical of a combined ELC and ECC process [6,7].

With increasing target thickness, charged (H^+) as well as neutral (H^0) components occur in the beam traversing the target. Accordingly, the observed spectra [Figs. 1(b)–1(d)] are the result of a mixture of convoy-electrons produced by charged and neutral projectiles. The shape of the convoy electron peaks depends on the evolution of both charge-state fractions along the projectile beam. It also depends on the electron scattering cross section σ_e (cm^2/at.) or mean free transport thickness λ_e (at./cm^2)$=\sigma_e^{-1}$ of the electrons in the target. Finally, when charge equilibrium is approached in the projectile beam, the spectra obtained with incident H^+ and H^0 [Fig. 1(d)] show almost the same shape, which then tends to become independent of any further increase of the total thickness π.

We now present a quantitative study of the evolution of the convoy-electron yields as a function of target thickness. For this purpose all the measured spectra, such as those seen in Fig. 1, were integrated from $v_p-\Delta v$ to $v_p+\Delta v$, centered at the velocity v_p of the peak maximum. Two different ranges $\Delta v=0.03$ and 0.003 a.u. were used. For the smaller range the integral can be considered to be representative of the peak height. Additionally, we evaluated spectra for three selected angular acceptances of the spectrometer, with half angles $\theta_0=0.25°$, 0.5°, and 1.0°. The reproducibility of the measured yields was within $\pm5\%$, and up to $\pm10\%$ for the smallest combined angular acceptance and range of integration.

We observed that the shape of the dependences with π of the yields does not depend within statistical error limits on the angular acceptance (θ_0) and integration limits ($v_p\pm\Delta v$). Consequently, we were able to merge them, by applying appropriate scaling factors, into the two yield dependences representative of incident H^0 and H^+. These scaling factors were determined using the respective mean count rates observed across the broad region of saturation found for target thicknesses from 10^{16} up to about 5×10^{16} atoms/cm^2. They were selected in such way that the saturation yields were normalized to one. We remark that only for the smallest thicknesses ($\pi=1.5\times10^{14}$ and 2.4×10^{14} at./cm^2), the dispersion of the so-obtained data did exceed the error limits of the individual yields. However, we did not, for $\theta_0=1°$, observe a systematic decrease of count rates in the region of low thicknesses, atributable to the fact that, in this case, the 0.75-mm-diam exit of our gas target cell imposes a quickly decreasing geometrical constraint on the effective angular acceptance for electrons emitted from the first 8 mm of this cell. Due to electron scattering in the gas target, the importance of this effect is obviously reduced.

In Figs. 2(a) and 2(b) we present our experimental yields as a function of π, for incident H^0 and H^+, respectively. For each of the 18 target thicknesses at which measurements were performed, we show the six experimental data points, obtained for the three angular acceptances and both integration ranges. In order not to produce superpositions, we desisted to assign differents symbols for each of the six combinations, limiting ourself to use crosses, the vertical and horizontal widths of which represent the statistical errors in yields and target thicknesses, respectively.

We now discuss the evolution of the yields $Y(\pi)$, shown in Fig. 2. Following Koschar *et al.* [9] and Barrachina *et al.* [10] (see also Ref. [4]), we write

$$Y(\pi)=\int_0^{\pi}d\pi'[F_0(\pi')\sigma_0+F_1(\pi')\sigma_1]\times\exp[-\sigma_e(\pi-\pi')]. \tag{3.1}$$

Here $F_0(\pi')$ and $F_1(\pi')$ describe the local charge fractions of neutral (0) and charged (1) projectiles as a function of the penetration (π') of the projectiles passing through the target of total thickness π. σ_1 and σ_0 are defined as the cross sections for production of convoy electrons by H^+ and H^0. σ_1 corresponds simply to the convoy electron production by the ECC process. σ_0 includes two channels: ELC from H^0 and ECC into a continuum state of H^0 [6,7]. The term in the first set of square brackets accounts for the local source of continuum electrons: At each position π' in the target we have a neutral $F_0(\pi')$ and a charged $F_1(\pi')$ beam component, each of which produces convoy electrons. The elimination from the measurement of part of these electrons by elas-

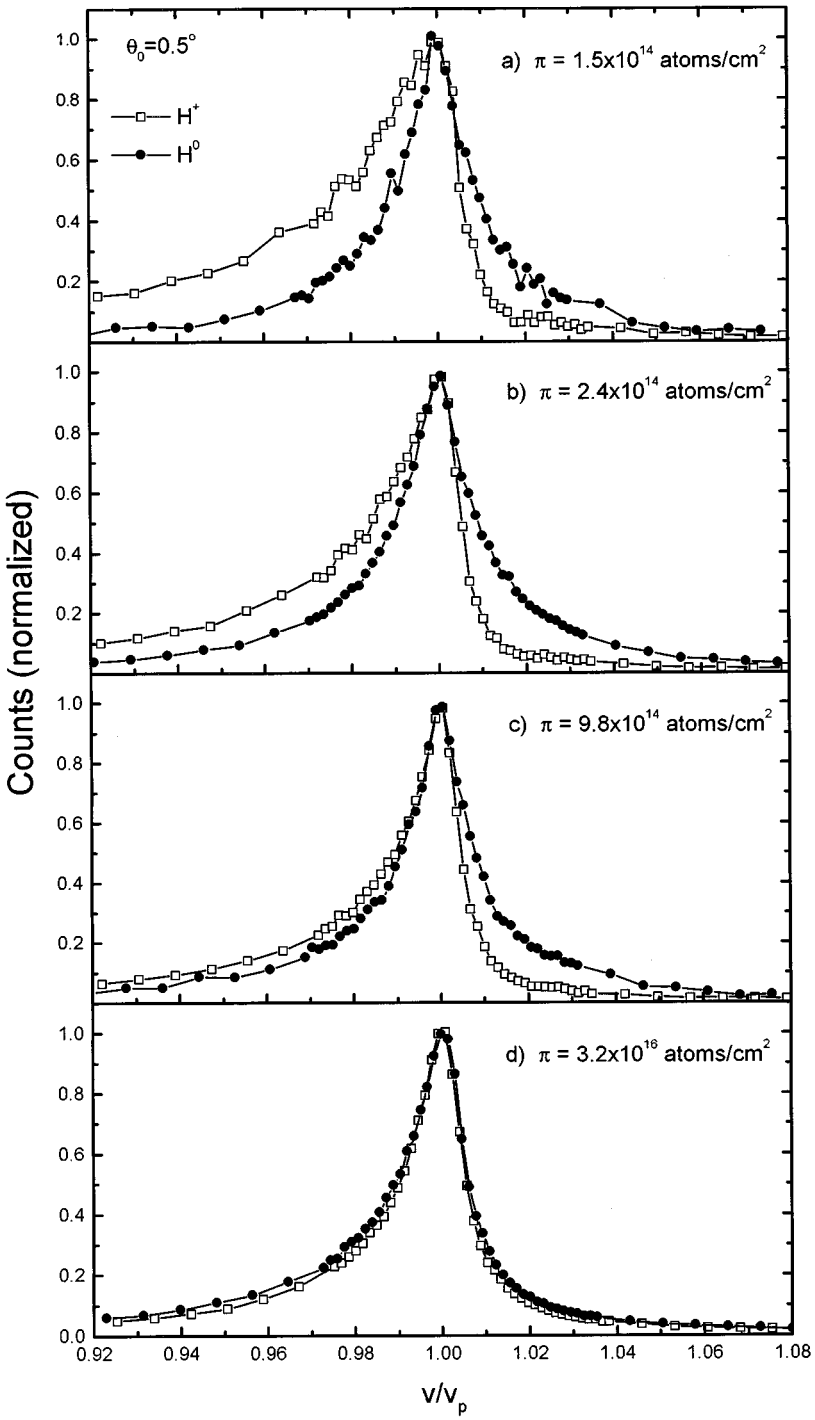

FIG. 1. Evolution of electron spectra for H^+ and H^0 for four target thicknesses π. The spectrometer angular acceptance was $\theta_0=0.5°$.

tic scattering is accounted for by the exponentially decaying term $\exp[-\sigma_e(\pi-\pi')]$, where σ_e is the elastic scattering cross section of the electrons and $(\pi-\pi')$ the distance in thickness from their place of birth to the target exit.

The charge fractions $F_i(\pi')$ $(i=0,1)$ can be written in terms of the total cross sections for electron capture into H^+ (σ_c) and for electron loss from H^0 (σ_l) as

$$F_i(\pi')=F_i(0)\exp(-\sigma\pi')+F_i(\infty)[1-\exp(-\sigma\pi')], \tag{3.2}$$

with $\sigma=\sigma_l+\sigma_c$. The charge equilibrium fractions can be expressed as $F_0(\infty)=\sigma_c/\sigma$ and $F_1(\infty)=\sigma_l/\sigma$ [10].

After integration, Eq. (3.1) reads

$$Y(\pi)=B\exp(-\sigma\pi)-(A+B)\exp(-\sigma_e\pi)+A, \tag{3.3}$$

$$A=\sigma_1[(\sigma_0/\sigma_1)F_0(\infty)+F_1(\infty)]/\sigma_e,$$

$$B=\sigma_1\{(\sigma_0/\sigma_1)[F_0(0)-F_0(\infty)] +[F_1(0)-F_1(\infty)]\}/(\sigma_e-\sigma).$$

Obviously, $A=Y(\infty)$ is the steady-state yield obtained for $\pi\to\infty$. Inspection of Eq. (3.3) reveals that the cross sections

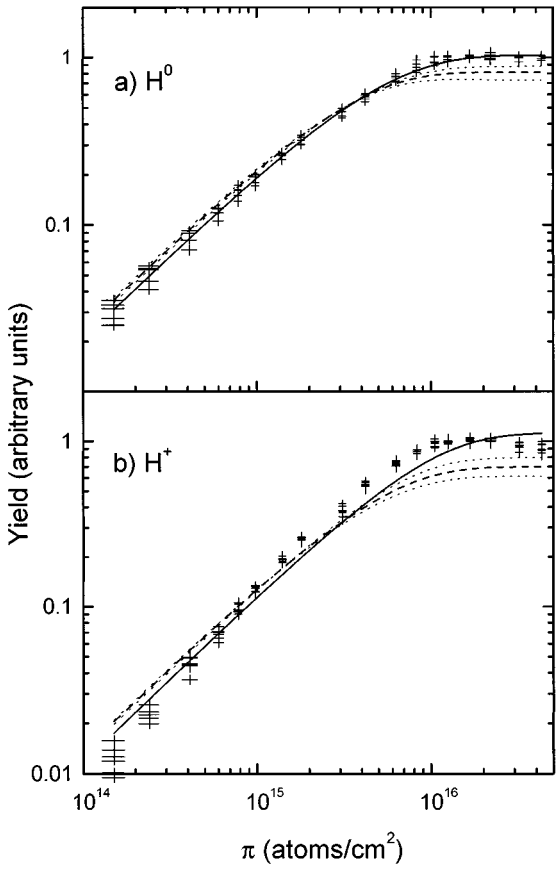

FIG. 2. Convoy electron yield as a function of target thickness for (a) H^0 and (b) H^+ incident projectiles. Experimental data are represented by crosses whose size corresponds to target thickness and yield uncertainties. Dashed lines, yield resulting for σ_e of free electrons; dotted lines, same as dashed lines, but including extreme quoted error limits for σ_l, σ_c, σ_e, and σ_0/σ_1 (see the text); full line, yield obtained with σ_{eff} (see the text).

σ_l, σ_c, and σ_e, together with the ratio σ_0/σ_1, determine the shape of the yield dependence $Y(\pi)$ as a function of the target thickness.

We now proceed to discuss possible systematic errors with reference to the integrated yields, due to simplifications implicit in the above model. In the first place the use of the total electron scattering cross section σ_e would imply that all the scattered electrons were eliminated from the measurement, a condition asymptotically fulfilled for $\theta_0 \to 0$. In fact, our electron spectrometer presents a finite acceptance in the solid angle, so we detect some of the scattered electrons. However, within experimental error limits, no systematic changes of the shape of the measured yield dependences were observed when we purposely changed the half angles of our angular acceptance cones ($\theta_0 =$ 0.25°, 0.50°, and 1.0°). This is a consequence of the fact that at velocities $v \approx v_p$ the differential cross section for electron scattering is such that almost all the electrons are scattered into angles larger than 1°.

We observed a slight shift of the peak maxima towards lower energies. The maximum of this shift was 0.16 eV for the thickest target used ($\pi = 4.3 \times 10^{16}$ at./cm^2) and is in accordance with known stopping cross sections of hydrogen projectiles in He [15]. Including in the integral of Eq. (3.1) the corresponding shift in energy as a function of the depth of origin of the convoy electrons in the target, only a negligible change in the calculated yields is obtained. Additionally we checked the relative importance of the angular ($\alpha_{1/2}$) and energy straggling (Ω) of the projectiles on the measured yields. From Refs. [16,17] we obtain for the maximum target thickness $\alpha_{1/2} = 0.08°$ and $\Omega = 0.160$ keV, which results in an energy straggling of 0.09 eV for the electrons. These effects were small compared to the angular and energy acceptance of our spectrometer.

For the comparison of the calculated yields in Eq. (3.3) with our experimental yields (Fig. 2) we employ published measured values for the cross sections: $\sigma_l = (1.23 \pm 0.15) \times 10^{-16}$ cm^2/at. [13], $\sigma_c = (1.34 \pm 0.40) \times 10^{-16}$ cm^2/at. [14], and $\sigma_e = (2.51 \pm 0.10) \times 10^{-16}$ cm^2/at. [12]. The ratio σ_0/σ_1 was obtained by means of an independent measurement using an effusive gas target, under single-collision conditions ($\pi \approx 10^{13}$ at./cm^2). We repeated this measurement with the three different angular acceptances and using the two specified ranges of integration, obtaining $\sigma_0/\sigma_1 = 1.5 \pm 0.2$.

In Fig. 2 we show the yields $Y(\pi)$, calculated from Eq. (3.3) (dashed lines), for incident H^0 [$F_0(0)=1$, $F_1(0)=0$] and H^+ [$F_0(0)=0$, $F_1(0)=1$]. For each curve a scaling factor was used as a fitting parameter. Two extreme curves (dotted lines) are also shown, as result of considering the uncertainties in the cross sections σ_l, σ_c, and σ_e and in the ratio σ_0/σ_1. Only approximate agreement with the experimental results is observed. Alternatively, when besides the abovementioned scaling factor also the electron scattering cross section σ_e is used as a free parameter, an improved agreement with the measured yields is obtained (full lines) with a decreased ''effective'' scattering cross section σ_{eff}, corresponding to an increased effective penetration depth $\lambda_{eff} = \sigma_{eff}^{-1}$. These results are shown in Table I. The uncertainties in σ_l, σ_c, and σ_0/σ_1 are taken into account to evaluate the uncertainty in σ_{eff}.

It is important to point out that an additional simplification of the model is that it considers monoenergetic electrons with an electron scattering cross section σ_e corresponding to the energy at the peak top. Contrarily, the experimental yield, defined by an integration of the measured spectra, includes a range of electron energies. The largest interval of

TABLE I. Free-electron scattering cross section σ_e and mean penetration thickness $\lambda_e = \sigma_e^{-1}$ from Ref. [12], compared to an effective scattering cross section σ_{eff} and penetration thickness λ_{eff}, as obtained by fitting the experimental yield dependences of Fig. 2.

Projectile	σ_e (10^{-16} cm^2/atom)	σ_{eff} (10^{-16} cm^2/atom)	λ_e (10^{15} atoms/cm^2)	λ_{eff} (10^{15} atoms/cm^2)
H^0	2.51±0.10	1.73±0.17	4.00±0.16	5.78± 0.58
H^+	2.51±0.10	1.33±0.15	4.00±0.16	7.52± 0.85

integration covered the range from 23.9 to 26.1 eV, within which the free-electron scattering cross section changes from $\sigma_e = 2.61 \times 10^{-16}$ to 2.41×10^{-16} cm^2/at. [12]. The smaller values of σ_{eff}, obtained for the best fit of the experimental data, are clearly outside these limits.

IV. DISCUSSION AND CONCLUSIONS

Let us take a closer look at the results obtained with incident H^0. For the smallest target thicknesses $\pi \leq 2.4 \times 10^{14}$ atoms/cm^2, using the cross section $\sigma_l = 1.23 \times 10^{-16}$ cm^2/atom [13] for projectile ionization, we find that $\pi\sigma_l/2 < 1.5 \times 10^{-2}$. Hence the condition for single collisions is well approximated. This is in accordance with the fact that the symmetric shape of the spectra shown in Figs. 1(a) and 1(b), which was characteristic for the above-mentioned superposition of ELC and ECC of neutral projectiles, is maintained for the smallest thicknesses. Furthermore, it is also in accordance with the initial slope of the convoy-electron yield dependence $Y(\pi)$, represented in Fig. 2(a) in doubly logarithmic scale, which is equal to one within experimental uncertainties, meaning that $Y(\pi)$ is proportional to π.

With increasing thickness π, projectiles of both charge states (H^0,H^+) are present in the target cell. An increasing contribution from ECC into H^+ manifests itself in a gradually increasing negative skewness of the measured cusps [Fig. 1(c)]. For $\pi \geq 3 \times 10^{16}$ this skewness ends up in a constant ratio of approximately 1.7:1 for the respective partial left-right half-widths (Fig. 1(d)]. Furthermore, as soon as the target thickness exceeds the effective transport thickness, $\lambda_{eff} = \sigma_{eff}^{-1}$ of the convoy electrons, the slope of $Y(\pi)$ begins to decrease gradually, then being predominantly determined by the evolution of the charge distribution in the projectile beam. Finally, it reaches saturation when charge equilibrium is attained at a thickness $\pi' = \pi - \lambda_{eff}$ inside the target.

The almost perfect fit of the experimental data obtained with incident H^0 when leaving the scattering cross section as a free parameter induces confidence in the applied model and the resulting value of σ_{eff} (or λ_{eff}). Contrarily, with incident H^+, the agreement is not so perfect. For the smallest thicknesses $\pi \leq 2.4 \times 10^{14}$ atoms/cm^2 and using the cross section for electron capture $\sigma_c = 1.34 \times 10^{-16}$ cm^2/atom [14], one obtains $\pi\sigma_c/2 = 1.6 \times 10^{-2}$. This value is small enough for a reasonable approximation to single collisions. However, we see in Figs. 1(a) and 1(b) that already for the smallest thicknesses there is a tendency to symmetrization. This effect is already remarkable for $\pi = 9.8 \times 10^{14}$ atoms/cm^2 [Fig. 1(c)]. The most immediate conclusion would be that already at these low thicknesses, a quickly increasing admixture of convoy electrons stemming from H^0 is present in the measured cusps. This is in agreement with the fact that in Fig. 2(b) the initial slope of the experimental yield is equal to about 1.2, instead of 1.0 as expected for single collisions. Accordingly for incident H^+ a satisfactory fit with the model leading to Eq. (3.3), which imposes single collisions at low target thicknesses, is not possible.

In order to account for the above-mentioned discrepancies, we used a three-component system by inclusion of metastable $2s$ states in Eqs. (3.1)–(3.3), but failed to improve the agreement with the experimental evidence observed with incident H^+. A tentative interpretation of this situation could be that σ_c includes capture into highly excited Rydberg states, the probability of which is comparable with that for ECC. Such Rydberg electrons can then be supposed to be ionized easily into the projectile continuum in a subsequent collision.

Summarizing our evidence, an experimental study of the emission of convoy electrons as a function of target thicknesses, including the transition from single-collision conditions up to the final saturation in shape and yield, has been performed with H^0 and, in a less definite manner, with H^+ of 45 keV, incident on a He gas target. We remark that the measurements of Koschar *et al.* [9], with 3-MeV H^0 and H^+ projectiles on carbon foils cover only a range of thicknesses whose lower limit, at which for incident H^+ a decrease to 80% of the saturation yield is obtained, is roughly equivalent to only 1.0×10^{16} atoms/cm^2 on our scale (Fig. 2).

The fact that we find an effective mean transport thickness λ_{eff} larger than λ_e, the transport thickness of free electrons, focuses attention on the influence of the Coulomb attraction by the charged projectile, ''felt'' by convoy electrons in solid foil targets. This subject has received considerable attention in the literature. Initially a mechanism of ''Coulomb focusing'' [18], acting upon the convoy electron as such, was tentatively supposed to be responsible for observed enhanced transport thickness. However, classical calculations, using stochastic dynamics [19], led to a more effective scattering of electrons by target atoms if they are exposed to the attraction of charged projectiles. The consequence of this effect, called ''Coulomb defocusing,'' means a reduction of the penetration of convoy electrons compared to that of free electrons. However, these same calculations led to cycles of transient trapping of these electrons into bound, preferably highly excited, Rydberg states of the projectile and subsequent release into the low lying projectile continuum states typical for convoy electrons. This dynamic mechanism of electron-ion correlation, characterized by an increased transport thickness of such ''entrained'' electrons [20], part of which is finally emitted as convoy electrons, does not include any of the properties typical for a solid target. Consequently, it is more justifiable to apply this argument to interpret the increased λ_{eff}, compared to λ_e of free electrons, observed in the present study of convoy-electron emission from thick gaseous targets. More experimental information with reference to convoy electrons from thick gaseous targets is desirable particularly at higher projectile energies, where the contribution from inelastic electron scattering is present. Then, also the enhanced cross section for electron loss would dominate the yield dependences.

ACKNOWLEDGMENTS

We would like to thank M.L. Martiarena for useful suggestions and discussions and R.O. Barrachina for a critical reading of the manuscript. This work has been partially supported by the Consejo Nacional de Investigaciones Científicas y Técnicas, Argentina.

[1] W. Meckbach and R. A. Baragiola, *Inelastic Ion-Surface Collisions* (Academic, New York, 1977), p. 283; V. H. Ponce and W. Meckbach, Comments At. Mol. Phys. **10**, 231 (1981).
[2] I. A. Sellin, in *Invited Papers of the Twelfth International Conference on the Physics of Electronic and Atomic Collisions, Gatlinburg, 1982*, edited by S. Datz (North-Holland, Amsterdam, 1982), p. 195; M. Breinig *et al.*, Phys. Rev. A **25**, 3015 (1982).
[3] K. O. Groeneveld, W. Meckbach, I. A. Sellin, and J. Burgdorfer, Comments At. Mol. Phys. **14**, 187 (1984).
[4] W. Meckbach and P. Focke, Nucl. Instrum. Methods Phys. Res. B **33**, 255 (1988).
[5] L. Sarkadi, J. Pálinkas, A. Köver, D. Berényi, and T. Vajnai, Phys. Rev. Lett. **62**, 527 (1989).
[6] X. Kövér, L. Sarkadi, J. Pálinkas, L. Gulyás, Gy. Szabó, T. Vajnai, D. Rerényi, O. Heil, K. O. Groeneveld, J. Gibbons, and I. A. Sellin, Nucl. Instrum. Methods Phys. Res. B **42**, 463 (1989).
[7] P. Focke, G. Bernardi, D. Fregenal, and W. Meckbach (unpublished).
[8] R. Latz, J. Schader, H. J. Frischkorn, K. O. Groeneveld, D. Hofmann, and P. Koschar, Z. Phys. A **304**, 367 (1982).
[9] P. Koschar, A. Clouvas, O. Heil, M. Burkhard, J. Kemmler, and K. O. Groeneveld, Nucl. Instrum. Methods Phys. Res. B **24**, 153 (1987).
[10] R. O. Barrachina, A. R. Goñi, P. Focke, and W. Meckbach, Nucl. Instrum. Methods Phys. Res. B **33**, 330 (1988).
[11] G. Bernardi, S. Suárez, D. Fregenal, P. Focke, and W. Meckbach, Rev. Sci. Instrum. **67**, 1761 (1996).
[12] D. F. Register, S. Trajman, and S. K. Srivastava, Phys. Rev. A **21**, 1134 (1980).
[13] S. Allison, Rev. Mod. Phys. **30**, 1137 (1958).
[14] M. E. Rudd, R. D. Dubois, L. H. Toburen, C. A. Ratcliffe, and T. V. Goffe, Phys. Rev. A **28**, 3244 (1983).
[15] J. F. Ziegler, J. P. Biersads and U. Littmark, *The Stopping and Range of Ions in Solids* (Pergamon, Oxford, 1985); STOP program with coefficients, 1995.
[16] P. Sigmund and K. B. Winterbon, Nucl. Instrum. Methods **119**, 541 (1974).
[17] E. Bonderup and P. Hvelplund, Phys. Rev. A **4**, 562 (1971).
[18] I. A. Sellin, J. Burgdörfer, S. D. Berry, M. Breinig, H. D. Betz, and K. O. Groeneveld, J. Phys. B **19**, L155 (1986).
[19] J. Burgdörfer and J. Gibbons, Phys. Rev. A **42**, 1206 (1990).
[20] Y. Yamazaki, L. H. Andersen, and H. Knudsen, J. Phys. B **23**, L317 (1990).